VIII International Conference on Computational Methods for Coupled Problems in Science and Engineering
COUPLED PROBLEMS 2019
E. Oñate, M. Papadrakakis and B. Schrefler (Eds)

HYBRID ANALYSIS FOR CONTINUA WITH SOLID AND LIQUID PROPERTIES IN INFINITE HIGH TUBES

M. GÖTTLICHER

Faculty of Civil Engineering and Conservation/Restoration
University of Applied Sciences Erfurt
99085 Erfurt, Gemany
e-mail: m.goettlicher@t-online.de, web page: http://www.fh-erfurt.de

Key words: Functional, Principle, Granular Material, Infinite Tube, Coupled Problems.

Abstract. Many materials like sand, soil, cement, snow and grain, perform like solids or liquids depending on loads and boundary conditions. The proposed coupled solid-liquid analysis has the potential to deal conveniently with the severe nonlinearities that are associated with single state descriptions. Linear elastic behavior characterizes the solid part. Slowly moving incompressible viscous behavior characterizes the liquid part.

1 INTRODUCTION

Granular material in structural and geotechnical engineering generally is treated as a solid with special reference to large deformations. Transformation to a steadily moving state is not possible. If granular material is treated as a liquid with special properties, the hydrostatic pressure evolves in the static state which is not in agreement with the observed impact on structures [2]. The internally coupled solid-liquid analysis presented in this paper allows the complete transformation between static solid state and steady liquid state.

The interaction of static solid and steady incompressible liquid continua has been discussed for an infinite high tube in 2004 [3]. A detailed approximation has been proposed in 2006 [4]. In the present paper the liquid state is represented by pressure only. Dependent on loads and boundary conditions an inhomogeneous distribution of solid and liquid properties in space results from the relation of the first stress invariants. The velocities may be determined in a secondary analysis.

2 FUNCTIONAL AND PRINCIPLE

A functional is postulated for plane continua [1, 5, 7] with solid and liquid properties:

$$\Pi = \frac{1}{2}\int_A \boldsymbol{\varepsilon}^T \boldsymbol{\sigma}_S \, dA - \int_A \mathbf{u}^T \mathbf{p} \, dA - \int_{B_b} \mathbf{u}^T \mathbf{b} \, dB + \mu \int_{B_m} \mathbf{u}^T \mathbf{Q}^T \boldsymbol{\sigma}_S \, dB + \int_{B_m} \mathbf{u}^T \mathbf{Q}^T \mathbf{c} \, dB \tag{1}$$

An elastic solid interacts with an incompressible liquid which is represented by a pressure field c.

$$\boldsymbol{\sigma}_S = \mathbf{E}\,\boldsymbol{\varepsilon} \tag{2}$$

The composite stresses consist of elastic stresses and pressure:

$$\boldsymbol{\sigma} = \boldsymbol{\sigma}_S + \mathbf{c} = \mathbf{E}\,\boldsymbol{\varepsilon} + \mathbf{c} \tag{3}$$

The first integral of the functional represents the elastic energy. The area load **p** in the second integral consists of the specific weight γ and the horizontal force p_2 that interacts between solid and liquid (Figure 1). The red variables describe the solid part. The blue variables describe the liquid part.

The third integral refers to the part B_b of the boundary, which is subjected to the load **b.** The boundary load consists of $\mathbf{b}_S$ acting on the solid part and **-c** acting on the liquid part.

$$\mathbf{b} = \mathbf{b}_S - \mathbf{M}^T\mathbf{c} \tag{4}$$

M Transformation matrix for loads

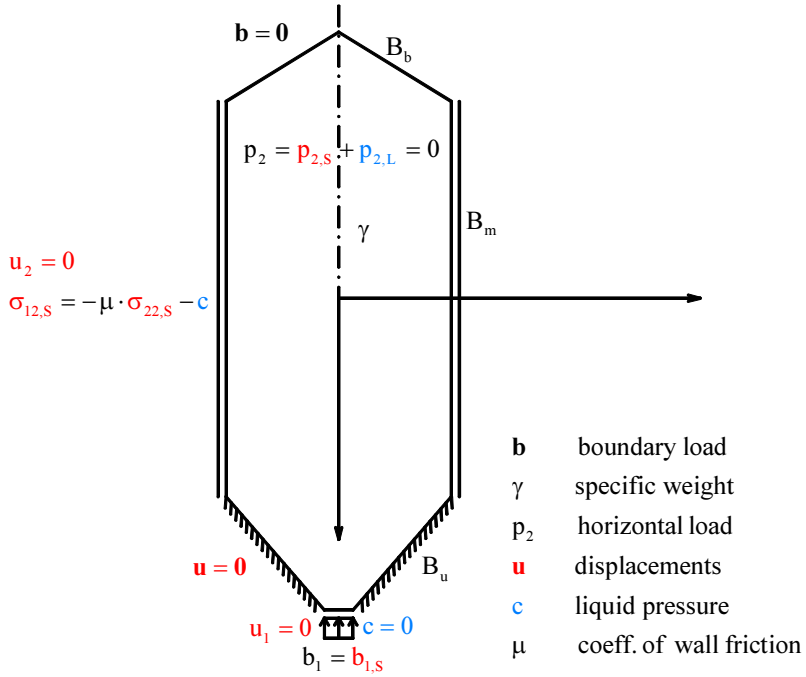

Figure 1: Displacements**,** pressure, loads and boundary conditions for the hybrid analysis of a silo

The last two integrals of the functional refer to the part B_m of the boundary, where slip is possible in the tangential direction. This part of the boundary is associated with a tangential force opposite to the direction of motion and results in a contribution to the internal virtual work. The lateral displacement is zero. Coulombs law determines the relation between stresses $\boldsymbol{\sigma}_S$ and load $\mathbf{b}_S$ for the solid part. Tension which would result in cavitation and the loss of bound is avoided for the liquid part by an appropriate relation between pressure **c** and load $\mathbf{b}_L$.

$$\mathbf{b} = \mathbf{b}_S + \mathbf{b}_L \tag{5}$$

$$\left.\begin{aligned} \mathbf{b}_S &= -\mu \mathbf{Q}^T \boldsymbol{\sigma}_S \\ \mathbf{b}_L &= -\mathbf{Q}^T \mathbf{c} \\ u_n &= 0 \end{aligned}\right\} \qquad \mathbf{x} \in B_m \qquad \operatorname{sign}(u_t) \tag{6}$$

Q Transformation matrix for interaction at the boundaries

At the remaining part B_u of the boundary the displacement **u** is zero.

$$B = B_b + B_m + B_u \tag{7}$$

The slip and stick parts of the boundary are determined a priori. The presented linearization requires a stationary motion at the walls. The validity of the a priori assumptions regarding boundaries and direction of motion are checked after the analysis and may lead to iteration.

The pressure field c becomes active if the displacement boundary conditions are not appropriate to maintain the equilibrium. Otherwise the pressure field vanishes, which results in a mere elastic analysis. The pressure c is assumed to be associated with an incompressible viscous slowly moving liquid that may be addressed in a secondary analysis.

$$\Pi = \frac{1}{2}\int_A \boldsymbol{\varepsilon}^T \mathbf{E} \boldsymbol{\varepsilon} \, dA - \int_A \mathbf{u}^T \mathbf{p} \, dA - \int_{B_b} \mathbf{u}^T \left(\mathbf{b}_S - \mathbf{M}^T \mathbf{c}\right) dB + \int_{B_m} \mathbf{u}^T \mathbf{Q}^T \left(\mu \mathbf{E} \boldsymbol{\varepsilon} + \mathbf{c}\right) dB \tag{8}$$

The functional covers the complete range from elastic static behavior to mere liquid behavior. It is restricted to applications without tension.

The variation of the displacements of the functional is set to zero. The pressure depends on the displacements for the prospective applications. It results the following hybrid principle:

$$\int_A \delta\boldsymbol{\varepsilon}^T \mathbf{E} \boldsymbol{\varepsilon} \, dA - \int_A \delta\mathbf{u}^T \mathbf{p} \, dA - \int_{B_b} \delta\mathbf{u}^T \left(\mathbf{b}_S - \mathbf{M}^T \mathbf{c}\right) dB + \int_{B_m} \delta\mathbf{u}^T \mathbf{Q}^T \left(\mu \mathbf{E} \boldsymbol{\varepsilon} + \mathbf{c}\right) dB = 0 \tag{9}$$

The derivations of the displacements determine the strains:

$$\boldsymbol{\varepsilon} = \mathbf{D}\mathbf{u} \tag{10}$$

$$\int_A \delta(\mathbf{D}\mathbf{u})^T \mathbf{E}(\mathbf{D}\mathbf{u}) \, dA - \int_A \delta\mathbf{u}^T \mathbf{p} \, dA - \int_{B_b} \delta\mathbf{u}^T \left(\mathbf{b}_S - \mathbf{M}^T \mathbf{c}\right) dB + \int_{B_m} \delta\mathbf{u}^T \mathbf{Q}^T \left[\mu \mathbf{E}(\mathbf{D}\mathbf{u}) + \mathbf{c}\right] dB = 0 \tag{11}$$

3 INFINITE HIGH TUBE

An infinite vertical tube is chosen as a representative application. These conditions are present for example in tall silos, in vertical blood vessels and in funnels of erupting volcanos.

For resting or steadily moving hybrid material in an infinite high tube, exact analytical solutions are available. This allows an evaluation of the general performance of the numerical analysis based on the hybrid solid-liquid formulation.

Figure 2 shows a horizontal slice taken from a vertical infinite high plane tube. The constant area load **p** which is identical to the specific weight γ acts on the material. With respect to infinity the complete weight of the slice is transferred to the vertical walls and results in shear forces that hold the equilibrium. Between the two walls the shear stresses vary linearly in the horizontal direction and stay constant in the vertical direction. The contribution of the cut off

upper and lower parts of the tube represents the related boundary load σ_{12} that acts on the top and bottom faces of the slice.
If no sliding is possible at the vertical walls the distribution of displacement is quadratic in the horizontal direction and constant in the vertical direction (Figure 2). The principal stresses are independent from the properties of the material. The major principal stress σ_I (compression) is opposite equal to the minor principal stress σ_{II} (tension). The angle is 45 degrees.
Since tension is not permissible for granular material a relative movement at the walls evolves.

3.1 Analysis

The link between the exact formulation and the approximate formulation is the analysis for nonlinear symmetric distributions of vertical stresses over the cross section (Figure 6). No changes regarding the vertical and horizontal stresses are possible in the vertical direction.

$$\frac{\partial \sigma_{11}}{\partial x_1} = 0 \qquad \frac{\partial \sigma_{22}}{\partial x_1} = 0 \qquad \frac{\partial \sigma_{22}}{\partial x_2} = 0 \tag{12}$$

No change of the vertical strain in the horizontal direction is possible since then the solid shear stresses would increase according to the infinity of the height.

$$\frac{\partial \varepsilon_{11}}{\partial x_2} = 0 \tag{13}$$

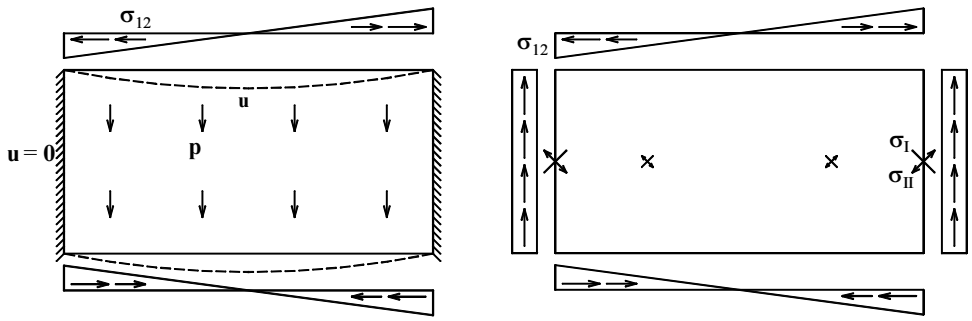

Figure 2: Fixed slice in an infinite high tube. **a**, area load, boundary load and deformation. **b**, shear stresses and principal stresses

Shear stresses follow from the equilibrium:

$$\sigma_{12} = -\gamma x_2 \tag{14}$$

Normal stresses:

$$\sigma_{11,S} = \sigma_{11} - c \tag{15}$$

$$\sigma_{22,S} = \sigma_{22} - c \tag{16}$$

$$\sigma_{22,S} = \frac{\nu}{1-\nu} \cdot \sigma_{11,S} \tag{17}$$

Boundary condition at the walls:

$$\sigma_{12} = c + \mu \sigma_{22,S} \tag{18}$$

Equilibrium at the walls:

$$\sigma_{12} = -\frac{\gamma L}{2} \tag{19}$$

3.2 Constant vertical stress distribution

Horizontal strain:

$$\varepsilon_{22} = 0 \tag{20}$$

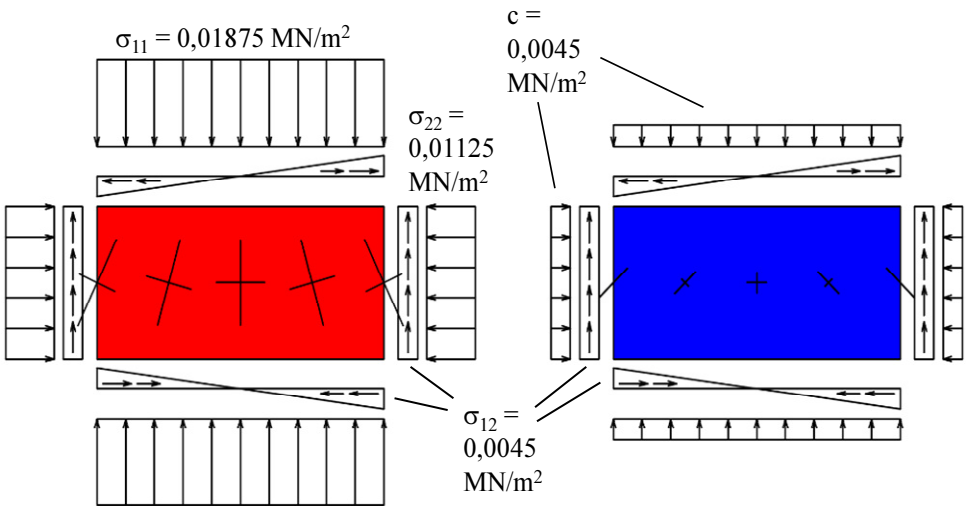

Figure 3: Boundary stresses and principal stresses in a slice of an infinite high vertical plane tube. **a**, elastic solid solution (left) and **b**, liquid solution (right)

Solid solution:

A mere solid solution evolves in the following case. The applied vertical boundary load b_1 causes horizontal stresses σ_{22} that activate shear stresses σ_{12} by wall friction that hold the equilibrium to the weight of the silo slice (Figure 3a).

$$\varepsilon_{11} = -\gamma L \cdot \frac{(1+\nu)(1-2\nu)}{2\mu E \nu} \tag{21}$$

$$\sigma_{11} = -\frac{\gamma L(1-\nu)}{2\mu \nu} \tag{22}$$

For a given height H of the solution area it is possible to determine the displacements. Index t refers to the top face; index b refers to the bottom face. Index c refers to the centre; index w refers to the walls.

$$u_{tc} = u_{tw} + u_{bc} \tag{23}$$

$$u_{tw} = \gamma H L \cdot \frac{(1+\nu)(1-2\nu)}{2\mu E \nu} \tag{24}$$

$$u_{bc} = \frac{\gamma L^2}{4E}(1+\nu) \tag{25}$$

3.3 Nonlinear vertical stress distribution

A nonlinear vertical stress distribution over the cross section is possible in an infinite high vertical tube. It probably will not evolve with respect to the minimum of elastic deformation energy.

Derivation of the stress strain relations:

$$\frac{\partial \varepsilon_{11}}{\partial x_2} = 0 \qquad \frac{\partial \sigma_{22}}{\partial x_2} = 0 \tag{26}$$

The integral of horizontal strain is zero according to the vertical tube.

$$\varepsilon_{22} = -\frac{1+\nu}{E} \cdot \sigma_{11} + c \tag{27}$$

$$\int_{-\frac{L}{2}}^{\frac{L}{2}} \varepsilon_{22} dx_2 = 0 = -\frac{1+\nu}{E} \int_{-\frac{L}{2}}^{\frac{L}{2}} \sigma_{11} dx_2 + cL \tag{28}$$

3.4 Functional and Principle

Functional:

$$\Pi = \frac{1}{2}\int_A (\mathbf{Du})^T \mathbf{E}(\mathbf{Du}) dA - \int_A u_2 \frac{\partial c}{\partial x_2} dA - \int_A u_1 \gamma dA - \int_{B_b} u_1 (b_1 - c) dB + \int_{B_m} u_1 \mu(\sigma_{22,S} + c) dB \tag{29}$$

Principle:

$$\int_A \delta(\mathbf{Du})^T \mathbf{E}(\mathbf{Du}) dA - \int_A \delta u_2 \frac{\partial c}{\partial x_2} dA - \int_A \delta u_1 \gamma dA - \int_{B_b} \delta u_1 (b_1 - c) dB + \int_{B_m} \delta u_1 \mu(\sigma_{22,S} + c) dB = 0 \tag{30}$$

4 APPROXIMATION

A fourth order approximation of the vertical displacement u_1 in the horizontal direction and a linear approximation in the vertical direction require six degrees of freedom with respect to the symmetry of the tube.

A single degree of freedom is required for a cubic approximation of the horizontal displacement u_2 since it is assumed to be constant in the vertical direction and to be zero in the center and at the walls of the tube. This degree of freedom is the horizontal strain $\overline{u}_2$ in the

center which is the first derivation of the horizontal displacement. The digits t and b of the nodal values refer to the top face and the bottom face (Figure 4).

$$\mathbf{u} = \mathbf{F}^{\mathrm{T}}\overline{\mathbf{u}} = \begin{pmatrix} \mathbf{f}^{\mathrm{T}} & 0 \\ \mathbf{0}^{\mathrm{T}} & \mathrm{f} \end{pmatrix} \cdot \begin{pmatrix} \overline{\mathbf{u}}_1 \\ \overline{\mathrm{u}}_2 \end{pmatrix} \tag{31}$$

Displacement at the walls:

$$\mathrm{u_w} = \mathbf{h}^{\mathrm{T}}\overline{\mathbf{u}}_{\mathrm{w}} = \frac{\mathrm{H} - \mathrm{x_1}}{\mathrm{H}}\mathrm{u_{tw}} + \frac{\mathrm{x_1}}{\mathrm{H}}\mathrm{u_{bw}} \tag{32}$$

Restriction of the vertical tube:

$$\mathrm{u_{bw}} = 0 \tag{33}$$

$$\mathrm{u_{tc}} = \mathrm{u_{bc}} + \mathrm{u_{tw}}$$

$$\mathrm{u'_{tw}} = \mathrm{u'_{bw}}$$

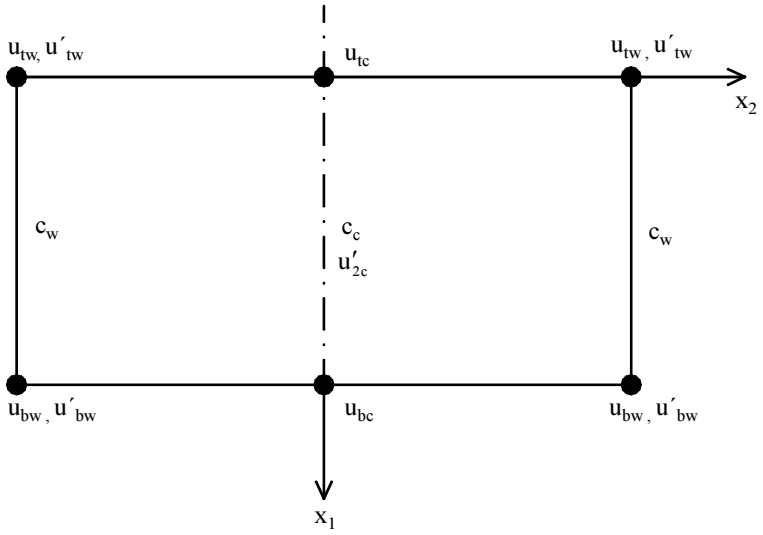

Figure 4: Nodal values for the interpolation functions

The liquid pressure c is assumed to be constant in the vertical direction and quadratic in the horizontal direction. Due to symmetry two degrees of freedom are required. These degrees of freedom are the liquid pressure c_c in the center and c_w at the walls (Figure 4).

Strain interpolation matrix:

$$\mathbf{B} = \mathbf{D}\mathbf{F}^{\mathrm{T}} \tag{34}$$

The boundary load **b** acts at the top face and the bottom face of the slice. The quadratic distribution of the vertical component b_1 depends on values b_c at the center and b_w at the walls. The linear distribution of the horizontal component b_2 depends on the value b_{2w} at the walls. It is zero in the center.

Integration of area load:

$$\int_A \mathbf{F}\,\mathbf{p}\,\mathrm{d}A = \begin{pmatrix} \gamma \int_A \mathbf{f}\,\mathrm{d}A \\ 0 \end{pmatrix} \tag{35}$$

The horizontal area load is an interaction between solid and liquid parts:

$$p_{2,L} = -p_{2,S} \tag{36}$$

Integration of partial area load:

$$\int_A \mathbf{F}\,\mathbf{p}_S \mathrm{d}A = \begin{pmatrix} \gamma_S \int_A \mathbf{f}\,\mathrm{d}A \\ -p_{2w,S} \int_A f\,g\,\mathrm{d}A \end{pmatrix} \tag{37}$$

$p_{2w,S}$ Solid part (S) of the horizontal force p_2 at the walls (w)

It follows with the principle (30):

$$\begin{aligned} &\delta\bar{\mathbf{u}}^T \int_A \mathbf{B}\,\mathbf{E}\,\mathbf{B}^T \mathrm{d}A\,\bar{\mathbf{u}} - \delta\bar{u}_2 \int_A f \frac{\partial \mathbf{g}^T}{\partial x_2} \mathrm{d}A\,\bar{\mathbf{c}} - \delta\bar{\mathbf{u}}_1{}^T \gamma \int_A \mathbf{f}\,\mathrm{d}A - \delta\bar{\mathbf{u}}_1{}^T \int_{B_b} \mathbf{f}\,\mathbf{g}^T \mathrm{d}B\left(\bar{\mathbf{b}}_1 - \bar{\mathbf{c}}\right) + \ldots \\ &\ldots + \delta\bar{\mathbf{u}}_w^T \mu \int_{B_m} \mathbf{h} \frac{\partial f}{\partial x_2} \mathbf{e}_2^T \mathbf{B}^T \mathrm{d}B\,\bar{\mathbf{u}} + \delta\bar{\mathbf{u}}_w^T \mu \int_{B_m} \mathbf{h}\,\mathbf{g}^T \mathrm{d}B\,\bar{\mathbf{c}} = \mathbf{0} \end{aligned} \tag{38}$$

5 EXAMPLES

Specific weight, Poisson's ratio and coefficient of wall friction in the applications represent grain [2]. The modulus of elasticity is chosen according to [6] (e.g. peat).

γ = 0,009 MN/m^2	specific weight
E = 1,000 MN/m^3	Young's modulus
ν = 0,375	Poisson's ratio
η = 0,001 MNs/m^2	viscosity
μ = 0,4	coefficient of wall friction
L = 1,00 m	width
H = 20,00 m	height

5.1 Constant vertical stress distribution

The finite element analysis reproduces the exact solutions for constant vertical stresses (Section 3.2). The stresses are negative for granular material since tension is not permitted. In the following discussion omits the sign for compression while (partial) tension is indicated by a minus sign.

Solid solution:

$$\sigma_{11} = 0,01875 \text{ MN} / \text{m}^2 \tag{39}$$

The solid solution represents the state of rest in a high silo.

The red color indicates the mere solid state of the hybrid material. Liquid pressure is zero. Solid stresses and displacements are identical with Section 3.2.

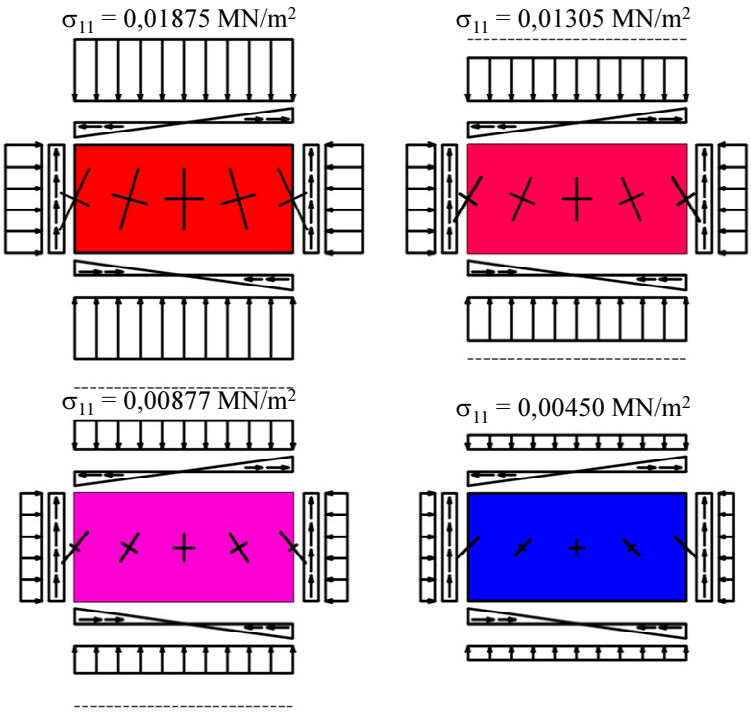

Figure 5: Transformation from **a**, the solid state (red) by the hybrid states (**b**, dark red and **c**, violet) to **d**, the liquid state (blue)

Liquid solution:

$$\begin{aligned} \sigma_{11} &= 0,0045 \text{ MN} / \text{m}^2 \\ \text{c} &= 0,0045 \text{ MN} / \text{m}^2 \end{aligned} \tag{40}$$

The blue color indicates the mere liquid state of the hybrid material. Solid stresses and displacements are zero.

The liquid solution evolves only for absent or nearly absent bottom since the flow velocity in the steady state is very high. For even higher velocities a granular gas evolves that is not covered by the performance of coupled solid and liquid analysis.

Hybrid solution:

The hybrid solid liquid solution represents the common situation in tall silos if the material is moving with a constant velocity. This happens sometime after the beginning of discharging. The behavior is primarily solid, and the velocity is small. No horizontal displacements evolve for constant vertical stress distributions.

Transformation:

The two states analysis enables the transformation from the static solid state at the beginning of time to the steady liquid state at the end of time. Figure 5 shows the solid and liquid states and two intermediate hybrid states.

The red picture in Figure 5 represents the solid state. The first violet picture represents an intermediate hybrid state. It contains more red color which indicates that the solid part dominates the liquid part. The second violet picture represents another hybrid state. It contains more blue color since the behavior is primarily liquid.

5.2 Quadratic vertical stress distribution

Nonlinear vertical stress functions σ_{11} result in nonlinear distributions of solid and liquid parts over the cross section. The relation between both parts is determined by the relation of the first stress invariants $I_{1,S}$ and $I_{1,L}$ (Table 1). Limiting condition for the solution area is that one part cannot exceed 100 %. According to Section 3.3 evolve horizontal area load p_2 and horizontal strain ε_{22}.

Table 1: Stresses, principal stresses, stress invariants, strains and horizontal load

Figure:	6a			6b		
x_2	0,5	0,25	0,0	0,5	0,25	0,0
σ_{11}	0,008775	0,001198	0,013050	0,007350	0,006281	0,005925
σ_{22}	0,010125	0,010125	0,010125	0,004650	0,004650	0,004650
c	0,000750	0,008766	0,011437	0,004400	0,001728	0,000837
p_2	0,042750	0,021375	0	-0,014250	0,007125	0
ε_{11}	0,00206	0,00206	0,00206	0,00241	0,00241	0,00241
ε_{22}	0,00392	0,00049	-0,00196	-0,00131	0,00016	0,00065
σ_{12}	0,00450	0,00225	0	0,00450	0,00225	0
σ_I	0,01400	0,01349	0,013050	0,010698	0,007859	0,005925
σ_{II}	0,00490	0,00862	0,010125	0,001302	0,003072	0,004650
α	40,7	33,8	0	36,6	35,0	0
$I_{1,L}/I_{1,S}$	0,793	0,079	0,987	0,733	0,316	0,158

Lower pressure in the centre:

Starting from the mere solid case only a decline of the vertical stresses in the center is possible to avoid tension. For lower vertical stresses in the center (Figure 6a) the partial solid stresses dominate in the center (red color). At the walls the liquid stresses finally exceed the solid stresses (violet color) If the vertical stresses in the center continue to decrease the solid stresses at the walls enter the not permitted tension range. This follows from the horizontal strain at the walls in the second column of Table 2.

Lower pressure at the walls:

Starting from the mere liquid case only an increase of the vertical stresses in the center is possible. For higher vertical stresses in the center (Figure 5b) the partial liquid stresses dominate in the center (blue color). At the walls the solid stresses finally exceed the liquid stresses (red color).

Transformation:

The mere solid solution (Figure 5a) turns to the hybrid solution (Figure 6a) if the constant stress function turns to a concave stress function. While the stress level decreases it approaches the mere liquid solution (Figure 5d). While the constant stress function turns into a convex stress function (which is barely possible) it turns to the hybrid solution (Figure 6b). While the stress level increases it finally approaches the mere solid solution again (Figure 5d).

Table 2: Transformation from the solid state (Fig. 5a) by the hybrid state (Fig. 6b) to the liquid state (Fig. 5d) and back to the solid state by the hybrid state (Fig. 6a), (x_2=0,5)

Fig.:	5a	6a	5d	6b	5a
$\sigma_{11,c}$	0,01875	0,013050	0,004500	0,005925	0,01875
$\sigma_{11,w}$	0,01875	0,008775	0,004500	0,007350	0,01875
σ_{22}	0,01125	0,010125	0,004500	0,004650	0,01125
c	0	0,000750	0,004500	0,004400	0
p_2	0	0,042750	0	-0,014250	0
ε_{11}	0,01031	0,00206	0	0,00241	0,01031
ε_{22}	0	0,00392	0	-0,00131	0
σ_{12}	0,00450	0,00450	0,00450	0,00450	0,00450
σ_I	0,020858	0,01400	0,004500	0,010698	0,020858
σ_{II}	0,009142	0,00490	0,004500	0,001302	0,009142
α	25,1	40,7	45,0	36,6	25,1
$I_{1,I}/I_{1,S}$	0	0,793	1,00	0,733	0

Table 2 shows the development at the walls (x_2 = 0,50 m) during this process. The intermediate states result from the development of the vertical stress in the center (x_2 = 0) in the first line.

6 CONCLUSIONS

The computational method presented in this paper covers a wide range of possible applications. It is based on the simultaneous interaction of two materials in the same place at the same time. The linearity of the analysis is preserved. The unavoidable nonlinear effects are covered by obvious a priori considerations as usual in engineering. Further research is directed

towards more general applications and the investigation of the usefulness of the numerical analysis that has been developed for an infinite high tube.

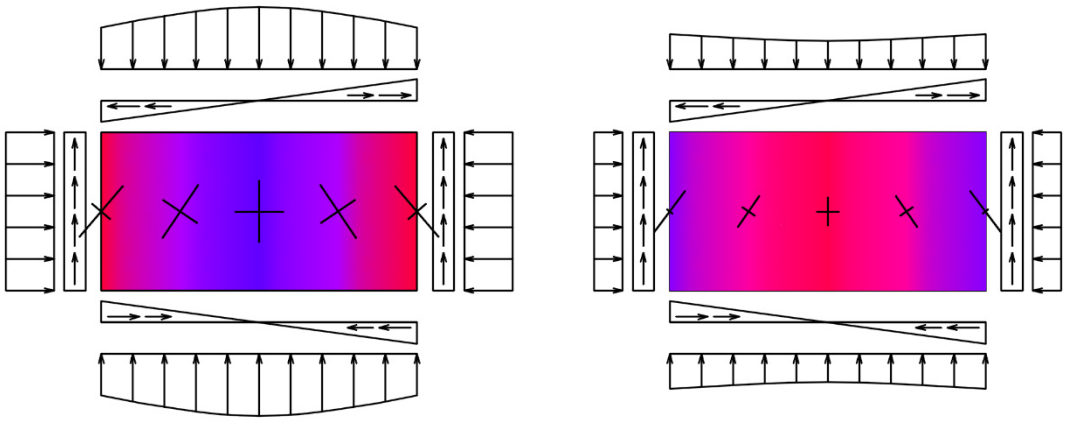

Figure 6: **a**, Primarily solid behavior at the walls and nearly liquid behavior in the center (left). **b**, Primarily liquid behavior at the walls and nearly solid behavior in the center (right).

REFERENCES

[1] KJ. Bathe, *Finite-Elemente-Methoden,* Springer-Verlag, (2012).

[2] S. Ehmann, K. Morgen, C. Ruckenbrod, *Silos.* Beton-Kalender, Band 2, Ernst & Sohn, (2016).

[3] M. Göttlicher, "*Flow of granular material in tall silos*", Proceedings of the sixth world congress on computational mechanics (WCCM), Abstract, Vol. 2, Springer-Verlag, (2004).

[4] M. Göttlicher, "*Hybrid solid-liquid model for granular material*", *17th international conference on the applications of computer science and mathematics in architecture and civil engineering (IKM), Bauhaus-University,* Weimar, Germany, (2006).

[5] K.A. Reckling, and P. Gummert, *Mechanik,* Springer-Verlag, (2014)

[6] J. Engel, *Geotechnik,* Bautabellen für Ingenieure. Bundesanzeiger Verlag, (2016).

[7] O.C. Zienkiewicz and R.L. Taylor, *The finite element method*, 5th Edition, Vol. 1, Butterworth-Heinemann, (2013).